Dynamic Light Scattering from Mixtures of Two Polystyrene Samples in Dilute and Semidilute Solutions

Julia Corrotto, Francisco Ortega, María Vázquez, and Juan J. Freire*

Departamento de Química Física, Facultad de Ciencias Químicas, Universidad Complutense, 28040 Madrid, Spain

Received May 30, 1995; Revised Manuscript Received June 12, 1996[⊗]

ABSTRACT: Static and dynamic light scattering experiments have been carried out for different solutions of two monodisperse polystyrene samples (with a ratio of molecular weights higher than 7) in toluene. We have investigated binary solutions (where the solute is one of the samples) and ternary solutions (where the solute is a mixture of the two samples) in relative concentrations so that both samples contribute similarly to the total scattered light. The total polymer concentrations range from the very dilute to the semidilute regimes. In the very dilute regime, the binary solutions yield the expected molecular weight dependence for the translational diffusion coefficients, while the dynamic scattering correlation functions for the ternary solutions can be deconvoluted into two independent contributions. In the semidilute regime, the correlation functions corresponding to the binary solutions are monoexponentials, showing a cooperative diffusional mode, due to local fluctuations in the polymer concentration. The dependency of hydrodynamic correlation lengths vs concentration clearly approaches the universal curve obeyed by other previously obtained data for semidilute systems. The semidilute ternary solutions exhibit a clear bimodal behavior. We observe a fast mode that can also be described as a cooperative diffusion coefficient (whose correlation length likewise falls into the universal curve). The slow mode is also diffusive, but the apparent diffusion coefficient shows a dependence with concentration opposite to that expected for the cooperative motion, approaching zero with increasing concentration. It is, in fact, an interdiffusional mode, due to the different chain lengths in the two samples. These experimental data are in quantitative agreement with the random phase approximation theory, developed by Benmouna et al. for several types of semidilute systems. The same theory is expected to also describe the dilute regime, if an appropriate modification is introduced to take into account hydrodynamic interactions between the chain segments.

Introduction

The study of the dynamic light scattering from nondilute polymer solutions has been a topic of growing interest in the recent past.[1] Experiments for semidilute solutions in solvents of various degrees of quality (Θ, good, and intermediate or marginal) have been carried out by different groups.[2−4] In the case of good solvents, most systems have shown a single-exponential decaying behavior for the experimental scattering correlation function. First-cumulant or other adequate fitting analysis of these results has been carried out, and the exponent values seem to be consistent with a cooperative diffusion coefficient, D_c, from which one can derive a hydrodynamic correlation length,[5]

$$D_c = k_B T/6\pi\eta_0\xi_h \qquad (1)$$

($k_B T$ is the Boltzmann factor and η_0 is the solvent viscosity).

Many data for solutions of polystyrene with different molecular weights can be plotted versus polymer concentration, c, in terms of a universal curve[6]

$$\xi_h\,(\text{nm}) = (0.53 \pm 0.10)c\,(\text{g/cm}^3)^{-0.70\pm0.01} \qquad (2)$$

This behavior can be justified with theoretical calculations based on the renormalization group theory.[7]

Ternary systems have also been investigated.[1] Usually, these studies use a "probe" of a given polymer in a "matrix" of another more concentrated polymer,[8,9] in order to obtain the translational diffusion coefficient of the probe. Polymers with a certain degree of compatibility, so that segregation is not important, have to be chosen for these experiments. Moreover, it is required that the solvent and the matrix have similar refractive indices, while the refractive index of the probe should be significantly different. In other experiments, the segregation effect is avoided by using samples of two different molecular weights of the same polymer.[10] In this case, two diffusive modes are expected; one of them represents the cooperative diffusion of the matrix, while the other one corresponds to the translational diffusion of the probe.

The results for ternary systems can be interpreted in the light of theoretical calculations performed by Benmouna et al.[11] These authors developed a random phase approximation theory and obtained results that can be applied to different situations. The results predict the general existence of two modes, one of them is that corresponding to local fluctuations in the total polymer concentration and, therefore, can be related with the correlation length by eq 1. The other mode describes the interdiffusion of the two types of chains, due to their differences in length.

This type of general approach seems to make possible the interpretation of semidilute solutions of ternary solutions, even when the concentration of the two types of chains does not follow the probe-matrix pattern. In particular, we believe that the investigation of systems where the ratio of concentrations between both types of polymers is constant can also be relevant. Considering the mixture of two different molecular weights has the additional advantage that one can easily set a ratio so that both samples contribute similarly to the total (or static) scattering density.

In this work we have performed static and dynamic light scattering measurements for this type of system; explicitly, we have measured mixtures of samples of polystyrene (PS) of two different molecular weights in

[⊗] Abstract published in *Advance ACS Abstracts,* July 15, 1996.

S0024-9297(95)00739-X CCC: $12.00

Table 1. Molecular Weight and Polydispersity of the Samples, According to the Manufacturers' Specifications, Together with the Determinations of Molecular Weights, Radii of Gyration, and Second Virial Coefficients from the Zimm Plots, As Explained in the Text, and Estimations of the Interpenetration Function and Overlapping Concentration, According to Eq 7

	PS-1	PS-2
From Manufacturers		
$10^{-5}M_w$ (g·mol^{-1})	7.06	0.964
M_w/M_n	1.05	1.01
From Our Zimm Plots		
$10^{-5}M_w$ (g·mol^{-1})	6.3 ± 0.6	0.88 ± 0.03
$\langle S^2\rangle_0^{1/2}$ (nm)	37 ± 2	12 ± 2
10^4A_2 (mL·mol·g^{-2})	4.9 ± 0.5	5.7 ± 0.5
ψ^*	0.28 ± 0.05	0.2 ± 0.1
10^3c^* (g·mL^{-1})	5.0	25
From an Empirical Equation[a]		
$\langle S^2\rangle_0^{1/2}$ (nm)	37.7	10.8
From the Ternary Solutions		
$10^{-5}M_{-1}$ (g·mol^{-1})	1.52 ± 0.03	
$\langle \bar{S}^2\rangle_0^{1/2}$ (nm)	27 ± 2	
$10^4\bar{A}_2$ (mL·mol·g^{-2})	5.1 ± 0.2	

[a] Reference 14: $\langle \bar{S}^2\rangle_0^{1/2} = (1.107 \times 10^{-2})M_w^{0.605}$.

the good solvent toluene. We have covered the region of total concentration ranging from very dilute solution to the semidilute regime. Since the difference in the molecular weight of the mixture is enough to allow us a deconvolution of dynamic data for dilute solutions in terms of two independent translational diffusion coefficients, another motivation of the present work has been to explore how these coefficients evolve in a continuous way in terms of total concentration, until they are transformed to the modes expected for the higher concentrations.

Experimental Section

Samples. We have used two samples of TSK standard polystyrene, purchased from TOSOH. The nominal weight-averaged molecular weights, M_w, and polydispersities of these two samples (hereafter PS-1 and PS-2) according to the manufacturers, are included in Table 1. It can be observed that the ratio of molecular weight is higher than 7, which should be high enough to allow for a clear separation of the modes corresponding to two different diffusion coefficients for the mixture in the dilute regime.

Solutions. The solvent used for preparing the solutions was toluene Carlo Erba, RPE type, (refractive index $n = 1.49$) which was filtered using 0.2 μm membranes and used without further purification. Solutions were prepared by weight, on an analytical balance of precision ±0.01 mg, directly in the cells. The scattering cells were cylindrical tubes made of quartz with 1 cm size and sealed with Teflon stoppers. The solutions were kept and manipulated always in a dust free environment. dn/dc was taken as 0.11 mL·g^{-1}.

After filtration the solutions were left to equilibrate for a period of days, depending on concentration, until reproducible results were obtained within the experimental uncertainty. In the case of the most concentrated solutions further tests were performed after longer periods of time (one or several months). These tests confirm the reproducibility of our earlier data.

We have prepared solutions with different concentrations for each one of the samples, and also for mixtures with relative compositions of the two samples so that they have similar contributions to the total scattering light, i.e. c(PS-1)M_w(PS-1) ≅ c(PS-2)M_w(PS-2).

Light Scattering Measurements. The light scattering experiments have been performed on a Malvern 4700 instrument, using the green line, $\lambda_0 = 514.5$ nm, of an Ar^+ ion laser Coherent I-70. We used the K7032 correlator equipped with 128 channels working in parallel mode that allow us to monitor simultaneously four to five time decades. The scattered intensity is obtained at each fixed angle through a 500 μm aperture by collecting 10 times the total number of photocounts during 10 s periods and averaging. Dark and solvent counts are subtracted, and the appropriate angle correction is performed.

Stability of the instrument was verified using the solvent toluene filtered through 0.2 μm membranes, in the angular range (30−145°) used for the static light scattering measurements. Deviations were found to be smaller than 1%. Toluene was also used as the standard reference for static measurements, assuming a Rayleigh factor of $R_v = 30.5 \times 10^{-6}$ cm^{-1}. This factor is obtained from the data reported in ref 12, that correspond to measurements with a 488 nm laser source, after a correction to take into account our values of n and λ_0 is introduced.

After preparation of samples with filtered toluene, no further filtration was needed in most of the non-very-dilute cases. Absence of dust was checked firstly by viewing the sample with cross polarizers. A stringent test was to record the light scattered at the lower angle of 30° for several hours. Samples with short-time deviations greater than 5% were rejected.

In the dynamic measurements, the solutions corresponding to all the ternary mixtures were measured at different scattering angles (in the range 30−140°). A similar range of angles was employed in all the static experiments. The dynamic measurements of binary solutions of a single sample were performed at 90°. However, a dilute solution of the PS-1 (highest molecular weight) sample was also observed at several angles. All measurements were performed at a temperature of 25.0 °C.

Analysis of Results

(a) Binary Solutions (PS-1 or PS-2 in Toluene). (a1) Static Scattering. The Zimm diagrams of binary solutions are included in Figure 1. In the case of the PS-1 sample at the highest concentrations, it can be observed that the angular dependence at a fixed concentration shows a clear upward curvature for the smallest angles. This effect can be expressed in terms of an interference function, depending on both angle and concentration, which departs from unity for some values of the angles, showing a minimum. A detailed description of these functions can be found in ref 13, where they are associated with high values of the term $[\eta]c$, combining intrinsic viscosity and concentration. This interpretation is in accordance with the present results, taking into account a previously reported empirical equation for the variation of intrinsic viscosity with molecular weight in PS/toluene systems[14] at 20 °C. (Assuming that the molecular weight in that equation can be substituted by M_w and ignoring temperature variations for an approximate estimation, we find that $[\eta]c \cong (1.069 \times 10^{-2})M_w^{0.724}c$ ranges from 0.05 to 2 for the prepared solutions.) The interference functions also affect the apparent slopes exhibited by all the nondiluted data of this sample, and the minimum reflects the liquidlike structure of the solutions near the overlap concentration. However, the increased slope observed for the highest concentrations of the PS-2 sample cannot be easily explained and it may have a purely experimental origin.

The angular dependence for the diluted solutions (at fixed concentration c) is fitted to the equation $Kc/\Delta R(\theta,c) = Kc/\Delta R(0,c)[1 + x/6]^2$, which is also employed to obtain zero-angle extrapolations. The averaged values of x so obtained can be identified with $x \equiv q^2\langle S^2\rangle = (4\pi n/\lambda_0)^2 \sin^2(\theta/2)\langle S^2\rangle$ for $x < 2.5$. This condition[13] is fulfilled by all the present data. This way we can obtain numerical values of the mean quadratic radius of gyration $\langle S^2\rangle$ for the most diluted solutions. In the case of the PS-2

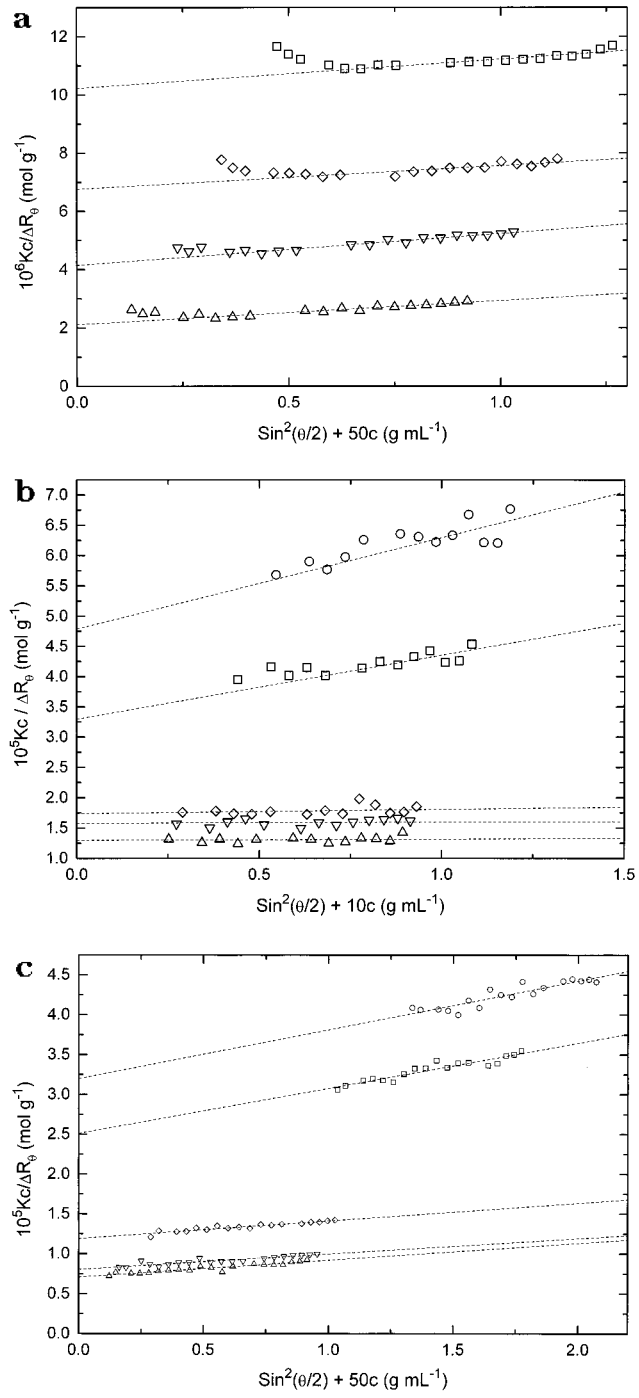

Figure 1. Zimm plots for the PS-1 sample (a), and PS-2 sample (b), and the mixtures (c). Values of the total polymer concentration, c (in 10^{-3} g·mL^{-1}); (1a) (△) $c = 0.757$, (▽) $c = 2.94$, (◇) $c = 5.02$, (□) $c = 7.64$; (1b) (△) $c = 1.02$, (▽) $c = 3.13$, (◇) $c = 4.83$, (□) $c = 19.9$, (○) $c = 30.4$; (1c) (△) $c = 0.632$, (▽) $c = 1.44$, (◇) $c = 8.05$, (□) $c = 23.8$, (○) $c = 39.9$.

sample, the angular dependence is very small for the dilute solutions, so that our results for $\langle S^2\rangle$ are obtained with high uncertainties and their change with concentration is within the experimental error bars. Nevertheless, we obtain $\langle S^2\rangle^{1/2} = 12 \pm 2$ nm. For the PS-1 sample, we obtain the value $\langle S^2\rangle_0^{1/2} = 37 \pm 2$ nm.

From the extrapolated values $Kc/\Delta R(\theta{=}0,c)$ obtained for the diluted solutions we have estimated the second virial coefficient, A_2, and weight-averaged molecular weights of the samples, M_w. These results, together with our estimations for the radius of gyration at low concentration, are included in Table 1. The molecular weights can be considered in agreement with the manufacturers specifications. Our results for the radius of gyration can also be compared with numerical values (also included in Table 1) obtained from these molecular weights, employing an empirical equation based on previous experimental measurements for dilute solutions of PS in toluene.[14]

The results for the second virial coefficient can be discussed in terms of the interpenetration factor ψ^*, obtained as

$$\psi^* = \frac{2A_2M^2}{(4\pi\langle S^2\rangle_0)^{3/2}N_A} \qquad (3)$$

(N_A is the Avogadro number, and M is the molecular weight of a chain, which we practically substitute for M_w). The results obtained for this magnitude are also included in Table 1. They are in agreement with previous data obtained for PS/toluene and other flexible polymers in good solvent,[15,16] $\psi^* \cong 0.2-0.3$.

(a2) Dynamic Scattering. The intensity time-correlation functions obtained in the correlator were directly analyzed by means of the standard deconvolution REPES[17] or CONTIN[18] programs, from which we obtain the distribution of relaxation times. Both programs give similar results in all the cases. For dilute solutions and low angles, we can essentially observe a single peak, corresponding to a mono-exponential correlation function. At higher angles, we observe another peak of considerably smaller (always less than 5%) amplitude at shorter times, which may indicate a second (faster) contribution. These features can be interpreted according to the Pecora theory[19] for dilute polymer solutions, directly based on the Rouse−Zimm model for single chain dynamics. The theoretical correlation function (proportional to the field time-correlation function, which is related to the intensity correlation function through the Siegert relation) can be expressed as a sum of exponentials of the type

$$P(q,\tau) = e^{-D_t q^2 \tau}[P_0(x) + P_{21}(x)e^{-2\tau/\tau_1} + ...] \qquad (4)$$

The terms $P_0(x)$, $P_{21}(x)$, etc., which characterize the amplitudes of the contributions, have a noticeable x dependence. For small values of x, $x \leq 1$, the first term predominates, and the chain translational diffusion coefficient, D_t, can be directly obtained. At higher values of x, however, we can find contributions of the internal modes. For the PS-1 solutions, the chain size is high enough to allow for the presence of a small second contribution of the form included in eq 4. However, its detection is in the limit of our experimental accuracy so that this second peak can also be a numerical artifact of the deconvolution procedure. An alternative first cumulant analysis yields a result that is in very good agreement with the slowest mode, i.e. $\Gamma \cong 1/\tau_{peak}$ in all cases. The results obtained from the cumulant analysis for a dilute PS-1 solution ($c = 3.55 \times 10^{-3}$ g/mL) at different angles are shown in Figure 2, where first cumulants are compared to the REPES values. A good agreement is observed, though the variance of the cumulant analysis systematically increases for increasing angles. The representation of Γ vs q^2 shown in Figure 2 indicates a clear linear, or diffusional, behavior. The slope obtained through a linear regression can be, therefore, identified with the mutual diffusion coefficient, $\Gamma = Dq^2$. This value of D is included in Figure 3, together with other results for

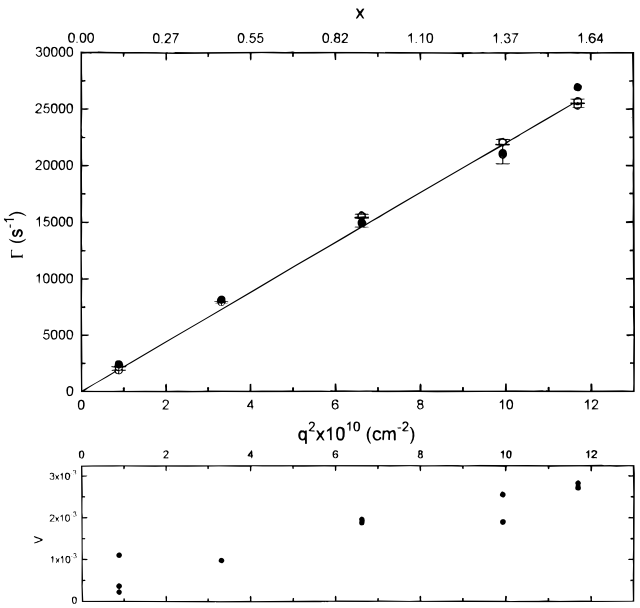

Figure 2. (Upper plot) Γ vs q^2 or x (upper scale) for a dilute PS-1 solution ($c = 3.55 \times 10^{-3}$ g/mL): (filled points) results from REPES (main peak); (open points) first cumulants; (solid line) linear fit. (Lower plot) variance v (from the ratio involving first and second cumulants) vs q^2.

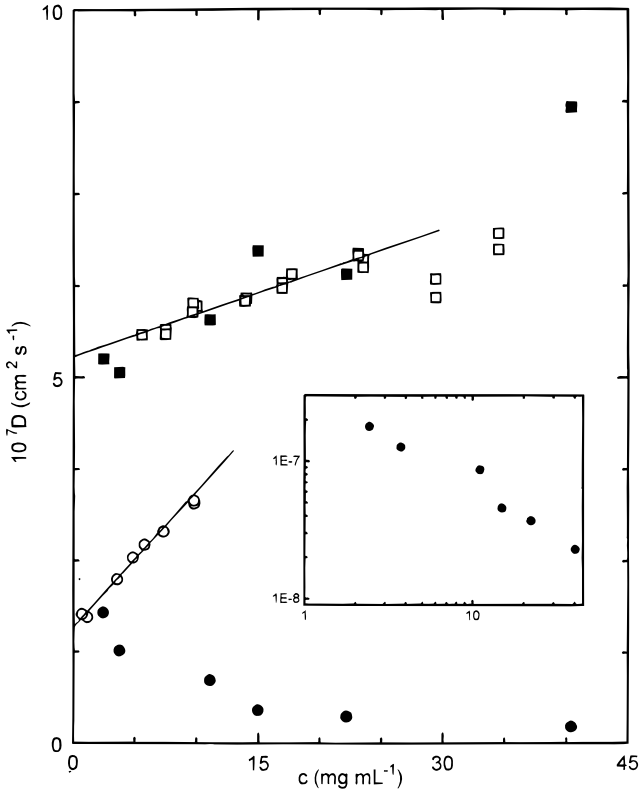

Figure 3. $D = \Gamma/q^2$ vs polymer concentration for binary solutions of the PS-1 (○) and PS-2 (□) samples, together with D_s (●) and D_f (■) vs total polymer concentration, obtained from the ternary mixture solutions: (solid lines) linear fits of D vs c in the dilute regime. Inset: logarithmic representation of the D_s data.

the same magnitude, similarly obtained from 90° measurements for the rest of PS-1 or PS-2 solutions at different concentrations. Nevertheless, we should mention that the mutual diffusion coefficient can only be obtained in the hydrodynamic limit and should only be identified as the slowest mode apearing at low values of q, in the case of nondilute solutions with structure.

Table 2. Dilute Solution Results for the Two Samples

	PS-1	PS-2
$D_0 \times 10^7$ (cm²·s⁻¹)	1.60 ± 0.05	5.30 ± 0.05
R_h (nm)	24 ± 1	7.4 ± 0.1
k_D (mL·g⁻¹)	116 ± 7	10.9 ± 0.7
ρ	1.54 ± 0.12	1.6 ± 0.3
From an Empirical Equation[a]		
$D_0 \times 10^7$ (cm²·s⁻¹)	1.56	5.11

[a] From ref 14: $D_0 = (3.64 \times 10^{-4})M_z^{-0.577}$. We assume $M_z \cong M_w$ for the present monodisperse samples.

However, the correlation functions of all the present binary solutions remain practically mono-exponential even for the highest concentrations. (As we have previously stated, a more detailed study at different angles is accomplished for the ternary solutions, the main goal of the study in the present work, and purely diffusional modes are obtained in all cases, as we will discuss below.)

The data shown in Figure 3 exhibit a linear behavior for dilute solution. Linear regression analyses in this region have allowed us to obtain results for the translational diffusion coefficient at infinite dilution, D_0, which are included in Table 2, together with the concentration coefficients, k_D, according to the equation

$$D = D_0(1 + k_D c) \tag{5}$$

The results for D_0 are in excellent agreement with the values obtained for the respective molecular weights according to an empirical equation obtained from previous ultracentrifuge measurements[14] of D_0 for very high molecular weight samples. As for the previously mentioned equations for $\langle S^2 \rangle$ and $[\eta]$, also reported in ref 14, this empirical equation is consistent with the exponential dependence with the molecular weight expected for dilute chains immersed in a good solvent, according to a theoretical scaling law.[20]

The results for k_D for several other polymer/solvent systems have been correlated with the corresponding concentration coefficient, k_f, obtained from measurements from ultracentrifuge measurements or other frictional properties,[1,21]

$$k_D = 2A_2M - k_f - \nu_2 \tag{6}$$

(ν_2 is the polymer partial specific volume, which in this case can be ignored since it is considerably smaller than the experimental uncertainties associated with k_D, M_w, and A_2). From eq 6 and our experimental values in Tables 1 and 2, we estimate $k_f = 500$ and 90 mL·g⁻¹ for the PS-1 and PS-2 samples. Ultracentrifuge results for other molecular weights of this system[14,22] at ca. 20 °C can be interpolated or extrapolated to the present case, and they give $k_f \cong 300$ and 80 mL/g, respectively. A previous dynamic light scattering study for dilute solutions of PS/toluene of two different samples[23] reported also slight discrepancies between extrapolated experimental values of k_f and the results obtained with eq 6.

The values for $\langle S^2 \rangle$ obtained from our Zimm plots or based on the empirical equation given in Table 1 can be compared with our experimental results for the Stokes−Einstein hydrodynamic ratio, R_h, defined from the relationship $R_h = k_BT/6\pi\eta_0D_0$. The values of $\rho = \langle S^2 \rangle_0^{1/2}/R_h$ for the two samples are included in Table 2. The results for ρ are higher than those corresponding to reliable experimental data[24] for PS in cyclohexane (Θ conditions). This increase in ρ is due to excluded-volume interaction effects and quantitatively agrees

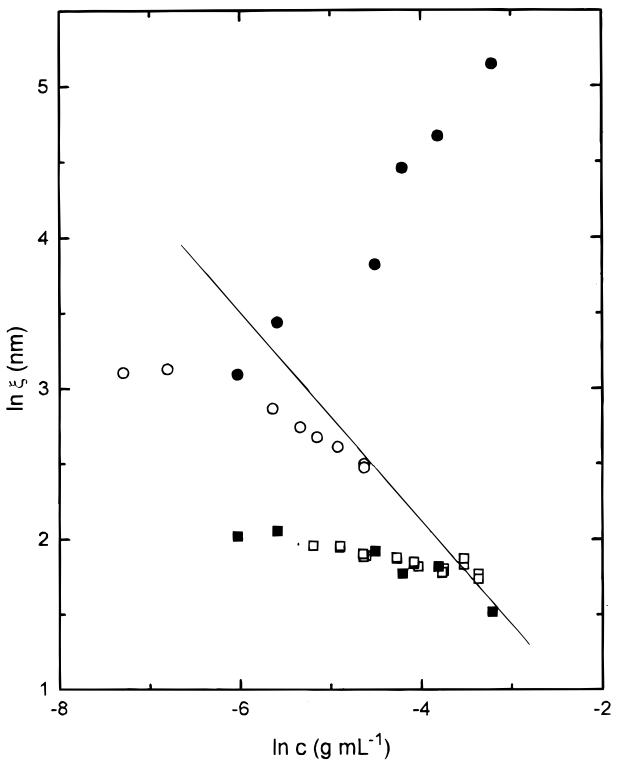

Figure 4. log−log representations of ξ_h vs polymer concentration for binary solutions with the PS-1 (○) and PS-2 (□) samples, together with similar representations for the apparent correlation lengths ξ_h^{app} (●) and ξ_h^{app} (■) described in text vs total polymer concentration for the ternary mixture solutions. The solid line is a representation of eq 2.

with numerical data obtained through Brownian dynamics simulations.[25]

As we mentioned in the Introduction, theoretical arguments and previous experimental work show that, in the pure hydrodynamic limit, the semidilute solutions of a monodisperse polymer in a good solvent should exhibit a single diffusive cooperative mode. The relaxation rate of this mode increases with polymer concentration, due to the decrease of the hydrodynamic correlation length (proportional to the monomer−monomer correlation length, or blob size). This cooperative mode describes the concentration fluctuations that relax by mutual diffusion between polymer units and solvent.[1,4,26] The behavior of our data in the semidilute range should be, therefore, consistent with this behavior, summarized by eqs 1 and 2. In order to confirm this point we have included the Figure 4 log−log plots of ξ_h (calculated from the diffusion coefficients) vs concentration for all the different solutions. It can be observed that the points corresponding to our most concentrated solutions tend clearly to agree with the universal curve. This indicates that the concentrations employed in this work cover the range from infinite dilution to the semidilute regime. In fact, a lower bound for the overlapping concentrations of both samples can be obtained as[26]

$$c^* = 3M_w/4\pi N_A\langle S^2\rangle_0^{3/2} \qquad (7)$$

Our estimations for the overlapping concentrations of the two samples are contained in Table 1. We can observe that these values are close to our upper concentrations. In fact the experimental points of the PS-1 sample fall on the universal curve at $c \cong 2c^*$. It can be considered, however, that the radius of gyration for the overlapping concentration are smaller as they start to approach those of nonexpanded chains, found at more concentrated solutions. Therefore, eq 7 tends to underestimate the actual value of c^* in the case of long expanded chains in dilute solution.

Table 3. Concentrations (in g·mL^{-1}) of the Two Polymer Samples in the Ternary Solutions, Values of $\nu = 2\bar{A}_2 M_{-1}c$, Together with the Contribution to Intensity of the Slow Mode in the 90° Measurements, a_s, and the Ratio D_c/D_i Obtained from the Correlation Functions and from Eq 13

solution	10^3c(PS-1)	10^3c(PS-2)	ν	a_s (%)	D_c/D_i[a]	D_c/D_i[b]
1	35.47 ± 0.05	4.92 ± 0.5	5.9	5	38 ± 6	30
2	19.32 ± 0.03	2.84 ± 0.03	3.2	10	17 ± 4	19
3	13.04 ± 0.02	1.92 ± 0.02	2.2	10	15 ± 2	14
4	9.65 ± 0.02	1.42 ± 0.02	1.6	15	7 ± 1	12
5	3.251 ± 0.006	0.481 ± 0.006	0.5	30	4.0 ± 0.6	8.3
6	2.151 ± 0.006	0.277 ± 0.006	0.35	30	2.9 ± 0.4	7.8

[a] Experimental. [b] From eq 13.

(b) Ternary Solutions (Mixtures of PS-1 + PS-2 in Toluene). As previously stated, the ternary solutions were prepared so that the PS-1 and PS-2 contribute similarly to the total scattered light. In Table 3, we show the concentrations of both samples in the different solutions prepared for the dynamic experiments. Similarly to our study of the binary solutions, we have determined the total scattering intensities corresponding to some ternary solutions, measured at different angles, obtaining a Zimm plot, which is included in Figure 1. In the range of low concentrations the interference function is not important[13] and, therefore, the analysis of this Zimm plot can be performed in terms of the general treatment for polymer mixtures in nondilute solutions proposed by Benoit and Benmouna.[27] In the present case of two samples of identical nature, the total scattering intensity can be expressed as

$$\frac{Kc}{I(q)} = \frac{c}{M_Ac_AP_A + M_Bc_BP_B} \times [1 + 2A_2^AM_Ac_AP_A + 2A_2^BM_Bc_BP_B] \qquad (8)$$

where we denote by subscript or superscript A and B the lowest and highest molecular samples, respectively. $c = c_A + c_B$ is the total concentration, A_2 is the second virial coefficient, and the q-dependent P_i represents the form factor of type-i chains. Furthermore, for values of x smaller than 1, we can set $P(q) = 1 - (1/3)q^2\langle S^2\rangle$. We also take advantage of the condition we have set to prepare these solutions. According to this condition the concentration ratio is approximately equal to the inverse ratio of molecular weights $c_A/c_B = M_B/M_A$, neglecting the actual small deviations with respect to this ratio. This way, eq 8 can be rewritten as

$$\frac{Kc}{I(q)} \cong \frac{1}{M_{-1}}[1 + (1/3)\langle\bar{S}^2\rangle q^2][1 + 2\bar{A}_2M_{-1}c] \qquad (9)$$

where

$$M_{-1} = 2/(M_A^{-1} + M_B^{-1}) \qquad (10)$$

$$\langle\bar{S}^2\rangle = [\langle S^2\rangle_A + \langle S^2\rangle_B]/2 \qquad (11)$$

and

$$\bar{A}_2 = (A_2^A + A_2^B)/2 \qquad (12)$$

We have fitted our most dilute solutions according to

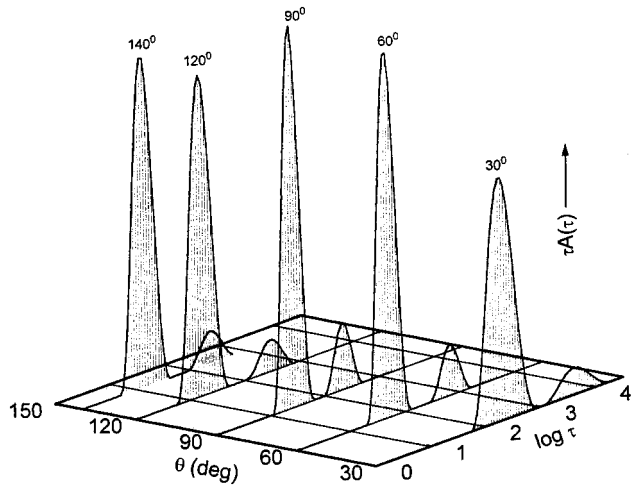

Figure 5. Scattering angle dependence of the relaxation time distribution function, $A(\tau)$, in an equal-area representation, obtained from REPES, for one of the ternary mixture solutions (solution 2).

eq 9, considering linear dependencies with q^2 but, otherwise, following the methods applied to the binary solutions. The results obtained from these Zimm plots according to eq 9 are included in Table 1 and are consistent with the results for the binary solutions, also included in the Table 1, and eqs 10−12.

The REPES analysis[17] for the dynamic light scattering correlation functions of the ternary solutions always yields a clear bimodal pattern. As an illustration, we include in Figure 5 the results obtained with one of the solutions (solution 2 in Table 3) measured at different angles. It can be observed that the relative amplitude of the slow and the fast mode peaks depends very weakly on the scattering angle. This weak dependence is also found for the rest of the nondiluted ternary systems here investigated. (The relative amplitudes of the slow mode, relative to their respective total intensities, obtained from the measurements at 90° for the different solutions are included in Table 3.) Moreover, when the numerical results for the location of slow and fast peaks, Γ_s and Γ_f, obtained for a given solution are represented vs q^2, we always obtained a linear dependence with negligible ordinate in the origin, similar to that shown in Figure 2 for the main contribution in dilute binary solution. Consequently, we find two diffusive modes for these solutions of mixtures.

The numerical linear regressions for Γ_s and Γ_f vs q^2 data yield slopes that we associate to apparent diffusion coefficients D_s and D_f. These values are incorporated in Figure 3, where they are represented vs c, which now represents the total polymer concentration. We can observe that the results for the highest diffusion coefficient (corresponding to the fast mode) are superimposed with the data corresponding to binary solutions prepared with the sample of lowest molecular weight in most of the concentration range. The results corresponding to the slow mode are also coincident with the data obtained from a solution with the highest molecular weight at very low dilution. This coincidence serves as a confirmation of the accuracy of the REPES numerical procedure to separate the modes. Thus, it is verified that the results for a very dilute mixture of the two samples can be deconvoluted to obtain two diffusion coefficients, and these coefficients are practically identical to those measured from very dilute solutions prepared separately with each one of the samples. At higher concentrations (even if for concentrations that still correspond to the dilute regime), the slow mode differs considerably from the cooperative diffusion coefficient of the longer chain. In fact, the apparent diffusion coefficients obtained for the slow mode in the mixtures decrease to zero with increasing polymer concentration, while cooperative diffusion coefficients increase with increasing c.

In Figure 4, we have also included the results obtained from the mixtures for an apparent hydrodynamic correlation length, obtained from the apparent diffusion coefficient as $\xi_i^{app} = kT/6\pi\eta_0 D_i$ (i = s or f), in a way consistent with the definition of ξ_h in eq 1. Again, we realize that the results from the fast mode seem consistent with a cooperative diffusion mode, associated with the local fluctuations of total polymer concentration. We can observe that the point corresponding to the most concentrated solution fits well into the universal curve, which serves as further confirmation of this point.

Clearly, the slow mode cannot admit a similar interpretation. At the intermediate and higher concentrations it should correspond to the relative motions of the two different types of chains, whose centers of masses diffuse at different rates and, therefore, describe the relaxation of the local relative concentrations (or interdiffusion) of the two polymer components.

Comparison with the RPA Theory

A quantitative analysis of the two modes can also be performed with the theory recently proposed by Benmouna et al., based on the random phase approximation.[11] This approximation consists of calculating the total intensity scattered by the different (two) polymer species in an incompressible mixture with a solvent taking into account the scattering of individual molecules and also considering the interactions between them. In the dynamical version of this theory, the response function to an external excitation is expressed as a time- and q-dependent density fluctuation of the two polymers. The density fluctuations are written in terms of bare response functions that contain the interactions between particles in terms of excluded volume parameters. The Laplace transform of this yields a system of linear expressions that define the actual response functions for the system. Finally, a generalized (matricial) Langevin equation is solved, neglecting memory effects. The application of this theory to the case of solutions of a mixture of two polymers only differing in their chain lengths predicts a dynamic light scattering time correlation function composed of two contributions. According to eq 42 of ref 11, the ratio between the apparent diffusion coefficients associated with the fast and slow (or cooperative, c, and interdiffusional, i) modes can be expressed as

$$D_c/D_i = \{(1 + 1/y + \nu) + [(1 - 1/y + \nu)^2 - 4\nu r(1 - 1/y)]^{1/2}\}/\{(1 + 1/y + \nu) - [(1 - 1/y + \nu)^2 - 4\nu r(1 - 1/y)]^{1/2}\} \quad (13)$$

where y is the ratio of the highest degree of polymerization to the lowest one. ν combines the usual excluded-volume parameter with the total concentration and can be described as $\nu = 2B_2c$, where $B_2 = A_2M$ is the second virial coefficient of the polymer, expressed in units of the inverse of concentration. In the original theory, it is assumed as a simplification that B_2 does not change with the chain length. For our case, it seems adequate

to identify ν with the second virial coefficient correction introduced for the total intensity in eq 9. This way, we set $\nu = 2\bar{A}_2 M_{-1} c$). Finally, r is the ratio of the volume fraction corresponding to the longest chain to the total polymer volume fraction.

In order to interpret the present experimental results by eq 13, we have set $y = M_w(\text{PS-1})/M_w(\text{PS-2}) = 7.324$. r can be estimated by assuming the same partial specific volume for both samples and volume additivity. This way, we can obtain r as the ratio of the highest molecular weight concentration to the total polymer concentration. This ratio varies slightly in the different measured solutions. However, we consider again this ratio as a constant value and adopt $r \cong M_w(\text{PS-2})/[M(\text{PS-1}) + M_w(\text{PS-2})] = 0.12$ as a single approximate value for all the solutions. Introducing our values for y and r into eq 13 and estimating ν from our experimental value for $\bar{A}_2$ and M_{-1}, we have obtained the ratios D_c/D_i. These theoretical predictions are compared with the experimental values obtained directly from the correlation functions in Table 3. A quantitative agreement is shown for the data corresponding to the moderately dilute and semidilute regimes. However, the experimental ratios are significantly smaller than those calculated with eq 13 in the case of the most dilute solutions. It should be pointed out that eq 13 yields for the infinitely dilute mixture ($\nu = 0$) the result $D_c/D_i = y$, identifying this ratio with the inverse ratio between molecular weights. This is consistent with the assignment of D_c and D_i to the individual diffusion coefficients of the lowest and highest molecular weight chains, provided that these coefficients can be described by the Rouse model. This picture is clearly in qualitative agreement with Figure 3. The Rouse model, employed for the formulation of the presently considered theory,[11] neglects hydrodynamic interactions, and consequently predicts diffusion coefficients that are inversely proportional to molecular weights. However, in order to give a good description of the dilute regime (and, therefore, to reproduce the experimental relation between the two values of D_0 and the molecular weights), one needs to introduce hydrodynamic interactions between polymer units. This way, the result for y would be consistent with the ratio of D_0 values. The latter values are actually related to the respective molecular weights through the scaling law mentioned in the discussion of the binary solutions, which also takes into account excluded-volume effects.[20]

Theoretical predictions for the relative amplitudes of the modes have also been reported (although they are explicitly available only in graphic mode). Then, they are shown as a function of r, and for the values $\nu = 1$ and 5, in Figure 2 of ref 11. Inspecting these graphic results and setting $r = 0.12$, we can expect a small amplitude (less than 5%) for the interdiffusional (or slow) mode with $\nu = 5$, while this amplitude increases to ca. 30% for $\nu = 1$. As we previously stated, we have found amplitudes that are practically independent of the scattering angle except for the two most dilute systems. The values of relative amplitudes of the slow mode in the semidilute regime contained in Table 3 for solutions 2 and 3 ($\nu \cong 2-3$), and for solution 1 ($\nu \cong 5$), seem to agree with the theoretical predictions.

Acknowledgment. This work has been supported by Grants PB92-0227 from the DGICYT (Spain) to J.J.F., and PB92-0200 from DGICYT and MAT93-1149-E from CICYT to F.O. We are also grateful to the Centro de Espectroscopía of the UCM for making available the light scattering facility.

References and Notes

(1) Brown, W., Ed. *Dynamic Light Scattering. The Method and Some Applications*; Clarendon Press: Oxford, U.K., 1993.
(2) Adam, M.; Delsanti, M. *Macromolecules* **1985**, *18*, 1760.
(3) Brown, W.; Johnsen, R. *Macromolecules* **1986**, *19*, 2002.
(4) Chen, S.-J.; Berry, G. C. *Polymer* **1990**, *31*, 793.
(5) Brochard, F.; de Gennes, P.-G. *Macromolecules* **1977**, *10*, 1157.
(6) Brown, W.; Nicolai, T. *Colloid Polym. Sci.* **1990**, *268*, 977.
(7) Shiwa, Y.; Oono, Y.; Baldwin, P. R. *Macromolecules* **1988**, *21*, 208.
(8) Wheeler, L. M.; Lodge, T. P. *Macromolecules* **1989**, *22*, 3399.
(9) Giebel, L.; Borsali, R.; Fischer, E. W.; Meier, G. *Macromolecules* **1990**, *23*, 4054.
(10) Brown, W.; Zhou, P. *Macromolecules* **1989**, *22*, 3508. Brown, W.; Zhou, P. *Macromolecules* **1989**, *22*, 4031. Brown, W.; Konak, C.; Johnsen, R. M.; Zhou, P. *Macromolecules* **1990**, *23*, 901.
(11) Benmouna, M.; Benoit, H.; Duval, M.; Akcasu, A. Z. *Macromolecules* **1987**, *20*, 1107.
(12) Bender, T. M.; Lewis, R. J.; Pecora, R. *Macromolecules* **1986**, *19*, 244.
(13) Berry, G. C. *Adv. Polym. Sci.* **1994**, *114*, 233.
(14) Appelt, B.; Meyerhoff, G. *Macromolecules* **1980**, *13*, 657.
(15) Huber, K.; Stockmayer, W. H. *Macromolecules* **1987**, *20*, 1400.
(16) Fujita, H. *Polymer Solutions*; Elsevier: Amsterdam, 1990.
(17) Jakes, J.; Stepanek, P. *Czech. J. Phys. B* **1990**, *40*, 97.
(18) Provencher, S. W. *Comput. Phys. Commun.* **1982**, *27*, 213. Provencher, S. W. *Comput. Phys. Commun.* **1982**, *27*, 229.
(19) Pecora, R. *J. Chem. Phys.* **1968**, *49*, 1032.
(20) Doi, M.; Edwards, S. F. *The Theory of Polymer Dynamics*; Clarendon: Oxford, U.K., 1986.
(21) Brown, W.; Zhou, P. *Macromolecules* **1991**, *24*, 5151.
(22) Mandelkern, L.; Flory, P. J. J. *Chem. Phys.* **1951**, *19*, 984.
(23) Pusey, P. N.; Vaughan, J. M.; Williams, G. *J. Chem. Soc., Faraday Trans. 2* **1974**, *70*, 1696.
(24) Schmidt, M.; Burchard, W. *Macromolecules* **1981**, *14*, 210.
(25) Rey, A.; Freire, J. J.; García de la Torre, J. *Macromolecules* **1991**, *24*, 4666.
(26) de Gennes, P.-G. *Scaling Concepts in Polymer Physics*; Cornell University Press: Ithaca, NY, 1979.
(27) Benoit, H.; Benmouna, M. *Macromolecules* **1984**, *17*, 535.

MA9507397